CHAPTER 25

FINITE-TIME LYAPUNOV EXPONENTS IN MANY-DIMENSIONAL DYNAMICAL SYSTEMS

TERUAKI OKUSHIMA

Department of Physics, Tokyo Metropolitan University, Minami-Ohsawa, Hachioji, Tokyo, 192-0397, Japan

CONTENTS

I. Introduction
II. Finite-Time Lyapunov Exponents and Vectors
III. QR Method and Its Correcting Procedure
  A. The Standard QR Method
  B. Finite-Time Error in QR Method
  C. Correcting Procedure for the QR Results
  D. Summary
IV. Lyapunov Instability in Many-Dimensional Hamiltonian Systems
  A. Order of Motion and Lyapunov Instability
  B. Coexistence of Qualitatively Different Local Instabilities
  C. Correction in Many-Dimensional Systems
  D. Summary
V. Conclusion
Acknowledgments
References

I. INTRODUCTION

The aim of this chapter is twofold. One is to give a new method for computing *finite-time* Lyapunov exponents and vectors in many-dimensional dynamical systems, and the other is to discuss the Lyapunov instability of a ϕ^4 model with this method.

Geometrical Structures of Phase Space in Multidimensional Chaos, Part B: A Special Volume of Advances in Chemical Physics, Volume 130, edited by M. Toda, T Komatsuzaki, T. Konishi, R.S. Berry, and S.A. Rice. Series editor Stuart A. Rice.
ISBN 0-471-71157-8

The spectrum of Lyapunov exponents provides fundamental and quantitative characterization of a dynamical system. Lyapunov exponents of a reference trajectory measure the exponential rates of principal divergences of the initially neighboring trajectories [1]. Motion with at least one positive Lyapunov exponent has strong sensitivity to small perturbations of the initial conditions, and is said to be chaotic. In contrast, the principal divergences in regular motion, such as quasi-periodic motion, are at most linear in time, and then all the Lyapunov exponents are vanishing. The Lyapunov exponents have been studied both theoretically and experimentally in a wide range of systems [2–5], to elucidate the connections to the physical phenomena of importance, such as transports in phase spaces and nonequilibrium relaxation [6,7].

The existence of Lyapunov exponents is proved, under a general condition, by the multiplicative ergodic theorem of Oseledec [8]. However, the convergence of the exponents is found to be quite slow (algebraically) in time for a generic dynamical system [9], due to its nonhyperbolicity.

In a nonhyperbolic system, chaotic and regular motions coexist, which induces large variations in the magnitudes of instability along a reference trajectory [10]. These variations are related to the alternations, *along a trajectory*, of chaotic and quasi-regular (laminar) motions in two-dimensional discrete-time dynamical systems [11], and further, that of random and cluster motions in high-dimensional Hamiltonian systems [12]. The variations of the instability can be quantified by *finite-time* Lyapunov exponents, which measure the exponential rates of principal divergences during *finite-time* intervals. Statistical scaling analysis of the distribution of finite-time exponents have revealed the presence of invariant structure in phase space, such as homoclinic tangencies [13]. Moreover, recent understandings of shadowability (i.e., computability of chaotic systems) [14,15], mixing process in two-dimensional incompressible flow, entropy production in advection-diffusion equation, and dynamo phenomena [16] have been widely developed with the essential use of finite-time Lyapunov exponents and vectors.

When a dynamical system is nonhyperbolic, there exist time intervals where part of the finite-time Lyapunov exponents accumulate around zero. Hence the spectra of the exponents are (quasi-)degenerate. These degenerate spectra impede our ability to obtain accurate numerical values of finite-time Lyapunov exponents using the existing numerical methods, namely, the QR method and the SVD method [9,17]:

1. The QR methods, based on the matrix factorization of QR decomposition [18], are effective and thus are widely used algorithms for computing the Lyapunov exponents [1,19–22]. However, for the *finite-time* Lyapunov exponents, these methods introduce errors that decrease only algebraically

in time [9]. Goldhirsch, Sulem, and Orszag have derived a correction for the standard QR method [9,23]. This correction is rather effective when the spectrum is nondegenerate, but insufficient to compute the accurate values of *finite-time* exponents when the spectrum is (quasi-) degenerate.

2. On the other hand, the SVD methods, based on the matrix factorization of singular value decomposition (SVD) [18], are algorithms, capable of computing accurate values of finite-time exponents [9,17]. However, the SVD methods not only have a practical disadvantage of requiring quite large computational costs, relative to QR method, but also have a severe limitation of being applicable only to continuous-time dynamical systems with nondegenerate Lyapunov spectra [17].

This chapter is organized as follows: Section II provides the basic definitions of Lyapunov quantities. In Section III, after summarizing the difficulty of the QR method, we construct a new method for computing accurate values of finite-time Lyapunov exponents, by generalizing the correction given by Goldhirsch et al. to higher-order corrections. We present the detail of our method, as well as discuss its efficiency with numerical confirmation. In Section IV, we apply this method to a many-dimensional ϕ^4 model and clearly show that qualitatively different local instabilities coexist along a trajectory and that the observation enables us to accurately determine lifetimes of ordered motions. The usefulness of our our method in many-dimensional systems is confirmed there. Section V summarizes this chapter.

II. FINITE-TIME LYAPUNOV EXPONENTS AND VECTORS

Let us consider continuous- or discrete-time dynamical systems in n-dimensional phase space $x = (x^1, x^2, \ldots, x^n)$, whose equations of motion are, respectively,

$$\frac{dx^j(t)}{dt} = f^j(x(t)) \quad \text{or} \quad x^j(t) = F^j(x(t-1)) \tag{1}$$

for $j = 1, 2, \ldots, n$. We write the solution of Eq. (1) starting from x_0 at $t = 0$, as $x(t, x_0)$. Then, the stability matrix from a time t_i to t_f along a reference trajectory $x(t, x_0)$ is given by the $n \times n$ Jacobian matrix $M(t_f, t_i; x_0)$ whose j–k element is defined as

$$M(t_f, t_i; x_0)_{j,k} = \frac{\partial x^j(t_f, x_0)}{\partial x^k(t_i, x_0)} \tag{2}$$

Here, an infinitesimal perturbation $v = (v^1, v^2, \dots, v^n)$ at $t = t_i$ is transformed to $M(t_f, t_i; x_0)\, v$ at $t = t_f$. It is noteworthy that $M(t_f, t_i; x_0)$ satisfies the relation

$$M(t_f, t_i; x_0) = M(t_f, 0; x_0)\, M(t_i, 0; x_0)^{-1} \tag{3}$$

The time-evolution equations of the stability matrix $M(t, 0)$ are the variational equation of Eq. (1), given by

$$\frac{dM(t,0)}{dt} = Df \cdot M(t,0) \quad \text{or} \quad M(t,0) = DF \cdot M(t-1,0) \tag{4}$$

where Df and DF denote the $n \times n$ Jacobian matrices of f and F evaluated at $x = x(t, x_0)$, respectively. The initial condition for Eq. (4) is $M(t = 0, 0) = I$, where I is the $n \times n$ identity matrix.

Now we introduce the finite-time Lyapunov exponents and corresponding vectors, utilizing the SVD of the stability matrix. The SVD of any $n \times n$ matrix, say A, is a matrix factorization [18]

$$A = U D V^T \tag{5}$$

where D is a diagonal matrix, and U and V are orthogonal matrices. These SVD matrices are constructed as follows: The symmetric matrix $A^T A$ has nonnegative eigenvalues $\{\sigma_j\}$ and the orthonormalized eigenvectors $\{v_j\}$. Defining u_j as

$$u_j = \frac{A v_j}{\mu_j} \tag{6}$$

with $\mu_j = \sqrt{\sigma_j}$ for $\sigma_j \neq 0$ and setting the other vectors u_j so that $\{u_j\}$ forms a orthonormalized bases set, we have $A = U D V^T$ with

$$D = \mathrm{diag}(\mu_1, \mu_2, \dots, \mu_n) \tag{7}$$

$$U = [u_1, u_2, \dots, u_n] \tag{8}$$

$$V = [v_1, v_2, \dots, v_n] \tag{9}$$

where $[u_1, u_2, \dots, u_n]$ denotes the matrix whose ith column vector is u_i.

Any matrix, and thus the stability matrix $M(t_f, t_i)$, is also factorized in the following SVD form:

$$\begin{aligned} M(t_f, t_i) &= U(t_f, t_i)\, D(t_f, t_i)\, V(t_f, t_i)^T \\ &= \sum_{j=1}^{n} u_j(t_f, t_i) \mu_j(t_f, t_i)\, v_j(t_f, t_i)^T \end{aligned} \tag{10}$$

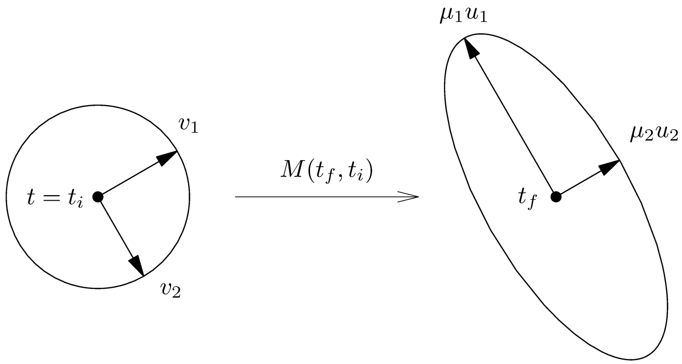

Figure 1. Graphic illustration of the singular value decomposition, Eq. (10), in a two-dimensional system.

where μ_j are, without loss of generality, assumed to be ordered as

$$\mu_1 \geq \mu_2 \geq \cdots \geq \mu_n \tag{11}$$

The meaning of the singular value decomposition, Eq. (10), is depicted in Fig. 1, which shows that the tangent vector v_j at $t = t_i$ is transformed to the tangent vector u_j multiplied by a scalar μ_j at $t = t_f$.

From this decomposition, the finite-time Lyapunov exponents in the time interval from t_i to t_f are given by

$$\lambda_j(t_f, t_i) = \frac{\log \mu_j(t_f, t_i)}{(t_f - t_i)} \qquad (j = 1, 2, \ldots, n) \tag{12}$$

The corresponding finite-time and left finite-time Lyapunov vectors are given by $v_j(t_f, t_i)$ and $u_j(t_f, t_i)$ in Eq. (10), respectively.

The ordinary (i.e., infinite-time) Lyapunov exponents and vectors are given by the $t_f \to \infty$ limits of the associating finite-time Lyapunov quantities:

$$\lambda_j = \lim_{t_f \to \infty} \lambda_j(t_f, t_i) \tag{13}$$

$$v_j(t_i) = \lim_{t_f \to \infty} v_j(t_f, t_i) \tag{14}$$

Here, the t_i-independency of the exponents is shown by the multiplicative ergodic theory of Oseledec [8].

III. QR METHOD AND ITS CORRECTING PROCEDURE

A. The Standard QR Method

The QR methods [1,19] are based on the relation

$$\lambda_j = \lim_{t\to\infty} \frac{\log R(t,0)_{j,j}}{t} \tag{15}$$

where $R(t,0)$ is the following matrix given by the QR factorization of the stability matrix:

$$M(t,0) = Q(t,0)\,R(t,0) \tag{16}$$

where the upper-triangular matrix $R(t,0)$ with nonnegative diagonal elements, as well as the orthogonal matrix $Q(t,0)$, is uniquely determined.

For a multidimensional chaotic system, the condition number of $M(t,0)$, which is defined by $\|M\| \times \|M^{-1}\|$ with $\|M\| := \max\{|Mx|/|x| \,:\, x \neq 0\}$ [18], becomes exponentially large for large t, which introduces a large amount of errors into the direct evaluation of Eq. (16) (orthonomalizing the column vectors in M).

To evade this numerical difficulty, the standard QR method evaluates Eq. (16) as follows [1,19]:

1. By dividing time into intervals τ ($t_k = k\tau$ for $k = 1, 2, \ldots$), $M(t,0)$ is represented as

$$M(t,0) = T_n T_{n-1} \ldots T_1 \qquad \text{for } t = n\tau \tag{17}$$

with

$$T_k = M(t_k, t_{k-1}) \tag{18}$$

2. Then, with utilizing QR decomposition repeatedly, Q_k and R_k ($k = 1, 2, \ldots$) are introduced as follows:

$$\begin{aligned} T_1 &= Q_1 R_1 \\ T_k Q_{k-1} &= Q_k R_k \qquad (k \geq 2) \end{aligned} \tag{19}$$

These matrices satisfy

$$M(t,0) = Q_n R_n R_{n-1} \ldots R_1 \tag{20}$$

and thus

$$R(t,0) = R_n R_{n-1} \ldots R_1 \tag{21}$$

3. The standard QR method evaluates the Lyapunov exponents as

$$\lambda_j = \lim_{t\to\infty} \frac{\sum_{k=1}^{n} \log(R_k)_{j,j}}{t} \tag{22}$$

since $\log(R(t,0)_{j,j}) = \sum_{k=1}^{n} \log(R_k)_{j,j}$ for upper-tridiagonal R_k.

B. Finite-Time Error in QR Method

We now introduce a normalized form of the stability matrix, which gives approximate values of finite-time Lyapunov exponents and vectors:

$$M(t_f, t_i) = Ue^d rV^T \tag{23}$$

where the dependencies, on t_i and t_f, of the matrices in the right-hand side are omitted for notational simplicity. Here, U and V are orthogonal, d is diagonal, and r is an upper-triangular matrix whose diagonal elements are normalized to unity. These matrices are determined as follows:

1. Since $M(t_f, t_i) = M(t_f, 0)M(t_i, 0)^{-1}$ and $M(t_n, 0) = Q_n R_n R_{n-1} \ldots R_1$, the stability matrix $M(t_f, t_i)$ is represented by

$$\begin{aligned} M(t_f, t_i) &= Q_f R_f R_{f-1} \ldots R_2 R_1 \cdot R_1^{-1} R_2^{-1} \ldots R_i^{-1} Q_i^T \\ &= Q_f R_f R_{f-1} \ldots R_{i+1} Q_i^T \end{aligned} \tag{24}$$

   where $t_i = i\tau$, $t_f = f\tau$. Therefore, U and V are chosen as

$$U = Q_f, \qquad V = Q_i \tag{25}$$

2. The remaining matrices d and r are, respectively, given by

$$d_{j,j} = \log(R_{i+1})_{j,j} + \log(R_{i+2})_{j,j} + \cdots + \log(R_f)_{j,j} \tag{26}$$

$$r = e^{-d} R_f R_{f-1} \ldots R_{i+2} R_{i+1} \tag{27}$$

   Practically, in order to obviate the numeric overflow or underflow, r is computed as

$$r = r_{f-i} \ldots r_2 r_1 \tag{28}$$

   where

$$r_1 = e^{-d_1} R_{i+1} \tag{29}$$

$$r_k = e^{-d_{k+1}} R_{i+k} e^{d_k} (k \geq 2) \tag{30}$$

and $(d_k)_{j,j} = \log(R_{i+1})_{j,j} + \log(R_{i+2})_{j,j} + \cdots + \log(R_{i+k})_{j,j}$. The estimations of U, d, and V are straightforward.

Note that if all off-diagonal elements of r are negligibly small compared to the diagonal elements, that is,

$$|r_{i,j}| \ll 1 \qquad \text{for} \quad 1 \leq i < j \leq n \tag{31}$$

then the jth finite-time Lyapunov exponent and (left) vector are given by $d_{j,j}/(t_f - t_i)$ and the jth column vectors of $(V)U$, respectively. Therefore, we define the QR-approximate exponents $\lambda^{\mathrm{QR}}(t_f, t_i)$ as

$$\lambda^{\mathrm{QR}}(t_f, t_i) = \frac{d_{j,j}}{(t_f - t_i)} \tag{32}$$

In general, however, r is far from diagonal, and thus λ^{QR}, U, and V are not accurate approximations of corresponding Lyapunov quantities.

To see the discrepancy between the exact and the approximate exponents, we have computed these values using the standard map (also referred to as the Chirikov–Taylor map):

$$\begin{aligned} y(t) &= y(t-1) - K\sin\left(x(t-1)\right) \\ x(t) &= x(t-1) + y(t) \end{aligned} \tag{33}$$

The exact exponents λ_j are directly computed by diagonalizing the symmetric matrix $M^T M$ with high-precision computation to evade its roundoff error. Figure 2 plots the error in the smallest exponents, $|\lambda_2^{\mathrm{QR}}(t,0) - \lambda_2(t,0)|$, against t. We can see that until $t \simeq 30$ the error rapidly decreases. After the initial dropping stage, it decreases slowly as $\sim 1/t$ (inset). This quite slow convergence shows that λ_j^{QR} is not a sufficiently accurate approximation of the finite-time Lyapunov exponent. Note here that behavior of λ_1 is similar to that of λ_2.

C. Correcting Procedure for the QR Results

Now we present our novel method for computing accurate values of finite-time Lyapunov exponents and vectors, by correcting the finite-time error in λ^{QR} [24].

To this end, we construct a sequence of refinements $U_{(k)}$, $d_{(k)}$, $r_{(k)}$, and $V_{(k)}$ $(k = 0, 1, 2, \ldots)$ satisfying

$$r_{(k)} \to \text{identity matrix} \qquad \text{as} \quad k \to \infty \tag{34}$$

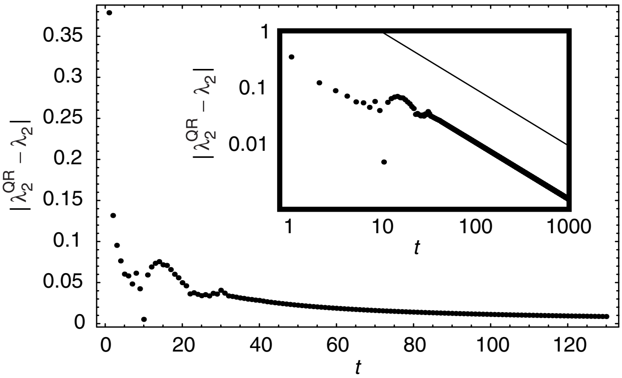

Figure 2. The finite-time errors in QR method, $|\lambda_2^{QR}(t,0) - \lambda_2(t,0)|$, are plotted against t. Semilog plot for $t < 130$ and log–log plot for $t < 1000$ (**inset**). In the inset, the solid line $10/t$ is shown for eye guidance.

with the normalization condition

$$M = \begin{cases} U_{(k)} e^{d_{(k)}} r_{(k)} {V_{(k)}}^T & \text{for even } k \\ U_{(k)} {r_{(k)}}^T e^{d_{(k)}} {V_{(k)}}^T & \text{for odd } k \end{cases} \tag{35}$$

Here $U_{(k)}$ and $V_{(k)}$ are orthogonal, $d_{(k)}$ is diagonal, and $r_{(k)}$ is an upper-triangular matrix whose diagonal elements are normalized to unity.

The construction of these matrices is as follows. Starting from $U_{(0)} = U$, $d_{(0)} = d$, $r_{(0)} = r$, and $V_{(0)} = V$, we generate the successors $d_{(k)}, r_{(k)}$ $(k \geq 1)$ by

$$\begin{aligned} {r_{(k-1)}}^T &= \mathscr{Q}_{(k)} \mathscr{R}_{(k)} \quad \text{(QRD)} \\ r_{(k)} &= e^{-d_{(k-1)}} \mathscr{D}_{(k)}^{-1} \mathscr{R}_{(k)} e^{d_{(k-1)}} \\ d_{(k)} &= \log(\mathscr{D}_{(k)}) + d_{(k-1)} \end{aligned} \tag{36}$$

where $\mathscr{D}_{(k)}$ is the diagonal matrix equal to the diagonal part of $\mathscr{R}_{(k)}$. The matrices $U_{(k)}$, $V_{(k)}$ are given by

$$U_{(k)} = U_{(0)} \mathscr{Q}_{(2)} \mathscr{Q}_{(4)} \cdots \mathscr{Q}_{(2\lfloor k/2 \rfloor)} \tag{37}$$

$$V_{(k)} = V_{(0)} \mathscr{Q}_{(1)} \mathscr{Q}_{(3)} \cdots \mathscr{Q}_{(2\lfloor (k-1)/2 \rfloor + 1)} \tag{38}$$

where $\lfloor x \rfloor$ denotes the largest integer not greater than x. As shown in Fig. 3, this procedure is intrinsically regarded as the diagonalization of the symmetric

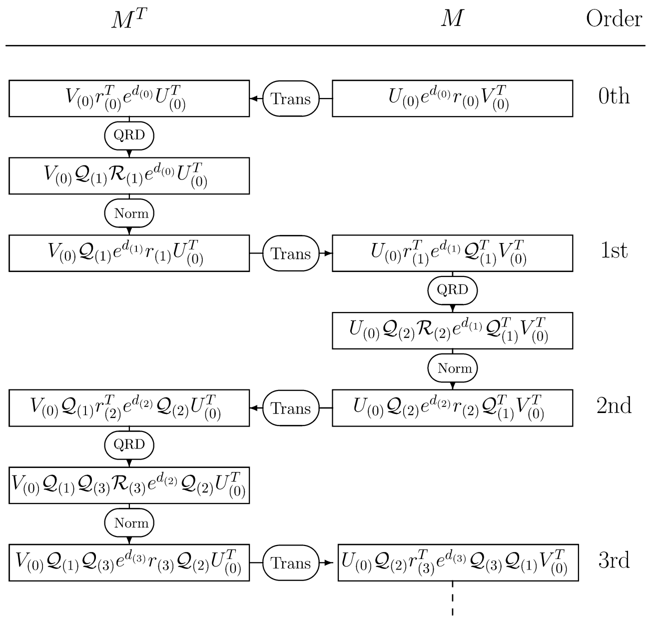

Figure 3. Diagrammatic representation of the correcting procedure Eq. (36), where "QRD" denotes QR decomposition of the matrix $r_{(k)}$ and "Norm" denotes the normalization procedure: $\mathscr{R}_k e^{d_{(k-1)}} \rightarrow e^{d_{(k)}} r_{(k)}$ (see text).

matrix $M^T M$ via the LR method [18], except for including the normalization for evading numerical disasters, arising from the large condition number of the stability matrix. From the general property of the LR method, we can see that this iterative procedure converges to the exact SVD exponentially as $k \rightarrow \infty$ [18]. Using $U_{(k)}$, $V_{(k)}$, and $d_{(k)}$, we define the kth corrected Lyapunov exponent as

$$\lambda_j^{(k)}(t_f, t_i) = \frac{d_{(k)j,j}}{(t_f - t_i)} \tag{39}$$

and the kth corrected (left) Lyapunov vectors as the jth column vector of $(U_{(k)})V_{(k)}$. Note that the first corrected exponent $\lambda_j^{(1)}(t,0) = d_{j,j}/t + \log(\mathscr{D}_{(1)_{j,j}})$ is equal to the correction derived by Goldhirsch et al. for nondegenerate spectra systems in Refs. 9 and 23. Namely, our correcting procedure is a generalization of the correction term proposed by them.

Here we numerically test our method using the standard map with the same parameters as in Fig. 2. The kth corrected errors in the smallest exponents, $|\lambda_2^{(k)}(t,0) - \lambda_2(t,0)|$, are plotted in Fig. 4a as a function of t for $k = 0, 1, 2,$

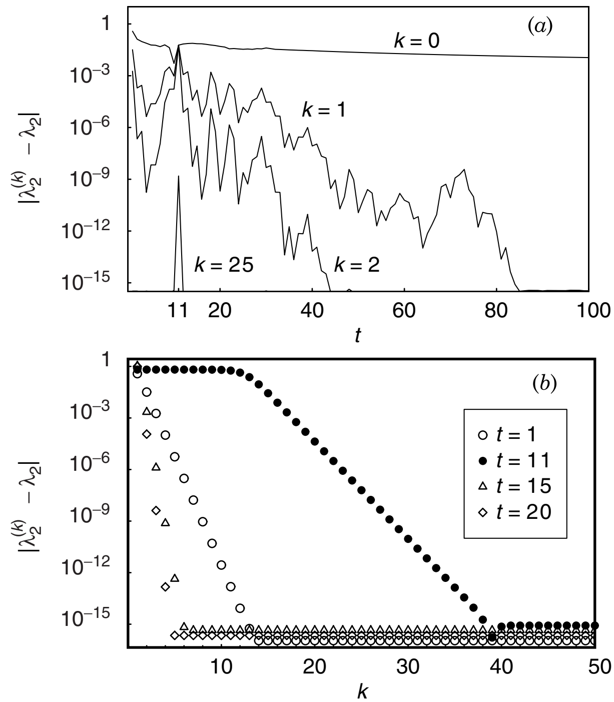

Figure 4. The kth corrected errors in the smallest exponents are plotted: (a) $|\lambda_2^{(k)}(t,0) - \lambda_2(t,0)|$ versus t for $k = 0, 1, 2$, and 25. (b) $|\lambda_2^{(k)}(t,0) - \lambda_2(t,0)|$ versus k for $t = 1, 11$, and 20.

and 25.[1] We can see that, for all t computed, the errors rapidly decrease as k increases, and we can also see that the convergencies have different rates dependent on t. For example, the slowest convergence is observed at $t = 11$. To see the detail of the convergencies, we plot the errors as a function of k in Fig. 4b. There are intervals of k in which the errors decrease exponentially, up to precisions close to the floating number precision (16 digits). At $t = 11$, the initial step k_0 at which the interval starts is larger ($k_0 \sim 15$) than that of $t \neq 11$ ($k_0 \sim 1$), because the standard QR method fails to describe the sudden changes in directions of Lyapunov vectors. This is the major reason for the slowest convergence observed at $t = 11$ in Fig. 4b. These observations show that the higher corrections ($k \geq 2$) are generally important for our high-accuracy computation of finite-time Lyapunov exponents.

[1]The behavior of λ_1 here is also similar to that of λ_2.

D. Summary

In this section, we have developed a numerical algorithm for computing accurate values of finite-time Lyapunov exponents and vectors, based on the standard QR method, by constructing a new correcting procedure. This correcting procedure is regarded as a generalized LR method. As a result, the correcting process exponentially converges to the exact Lyapunov quantities, and is, in contrast to the existing method, applicable for general dynamical systems, even when their Lyapunov spectra are (quasi-)degenerate or they are nonhyperbolic systems. This method is, as a whole, very efficient, because of the rapid convergence, and because the correcting procedure is only called when the exact quantities are necessary. Another virtue of this method is a practical advantage of being easy to implement [see Eqs. (19) and (36)].

IV. LYAPUNOV INSTABILITY IN MANY-DIMENSIONAL HAMILTONIAN SYSTEMS

In this section, we study the singular values of an many-dimensional oscillator system, as the first step toward the elucidation of the dynamical origin of ordered motions, and show a clear evidence of coexistence of qualitatively different local instabilities along a trajectory, which enables us to accurately determine lifetimes of ordered motions.

A. Order of Motion and Lyapunov Instability

Let us consider a $(2\Lambda + 1)$-degrees-of-freedom oscillator system (Λ is a nonnegative integer), whose Hamiltonian is given by a ϕ^4-interaction model truncated in reciprocal space (ϕ^4 MTRS):

$$H = \sum_{j=-\Lambda}^{\Lambda} \left(\tfrac{1}{2} p_j p_{-j} + \frac{\omega_j}{2} q_j q_{-j} \right) + \frac{\lambda}{4} \sum{}' q_{j_1} q_{j_2} q_{j_3} q_{j_4} \tag{40}$$

where $\omega_j = \sqrt{1 + j^2}$ and λ is a nonlinearity parameter. Here, all modes $j = -\Lambda, -\Lambda + 1, \ldots, \Lambda$ satisfy the reality conditions $q_j = q^*_{-j}$; $p_j = p^*_{-j}$ and

$$\sum{}' = \sum_{j_1, j_2, j_3, j_4 = -\Lambda}^{\Lambda} \delta_{j_1 + j_2 + j_3 + j_4, 0} \tag{41}$$

For the ϕ^4 MTRS with $\lambda = 1.0$ and $N(= 2\Lambda + 1) = 5$, we compute the finite-time Lyapunov exponents $\lambda_j(t, t - \Delta T)$ with $\Delta T = 1000$, via the corrected QR method developed in the previous section. The initial condition

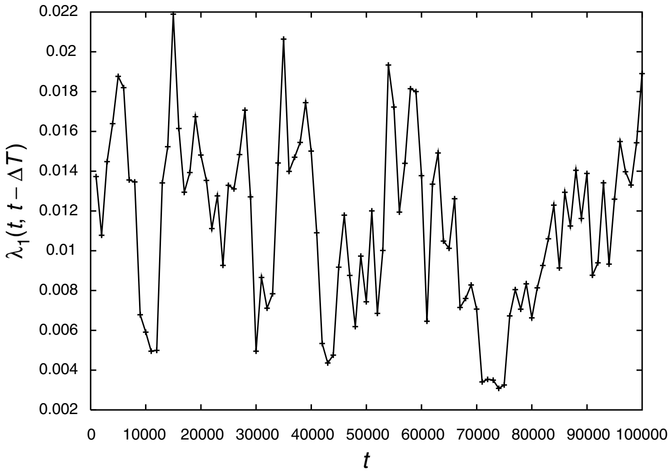

Figure 5. Plot of $\lambda_1(t, t-\Delta T)$ against t with $\Delta T = 1000$ for ϕ^4 MTRS.

has total energy 200 where the action variables are set to have ratio

$$I_{-2} : I_{-1} : I_0 : I_1 : I_2 = 2 : 0 : 1 : 3 : 1 \tag{42}$$

and the angular variables are given by random numbers form uniform distribution in $[0, 2\pi)$. (The following arguments are independent of the random number realizations.)

Figure 5 shows that the leading exponents are positive and thus the ϕ^4 MTRS is chaotic. In addition, they varies depending on the time intervals: We see relatively small instability regions, for example, around the intervals 9000–12,000 and 70,000–75,000. The variations of finite-time Lyapunov exponents have been related to the alternations between qualitatively different motions, such as (a) chaotic and quasi-regular, laminar motions in two-dimensional systems [11] and (b) random and cluster motions in high-dimensional systems [12], and they have been utilized for detecting these ordered motions.

Let us confirm the correspondence between the relative magnitude of instability and the orders of motions with this ϕ^4 MTRS. Figure 6 shows stroboscopic data of $j = 0$ mode variables (x_0, p_0) with sampling period $1/\omega_0$. The left panel presents the data in the time interval $70{,}000 \leq t \leq 75{,}500$, where the leading finite-time Lyapunov exponent is relatively small. A coherent, quasi-periodic motion is clearly seen in these variables. Since almost all energy concentrates in the zeroth mode, the other mode variables $j \neq 0$ are hardly excited in this coherent motion. In contrast, the right panel in Fig. 6 presents the data in the time interval $20{,}000 \leq t \leq 25{,}500$, where the leading exponent is

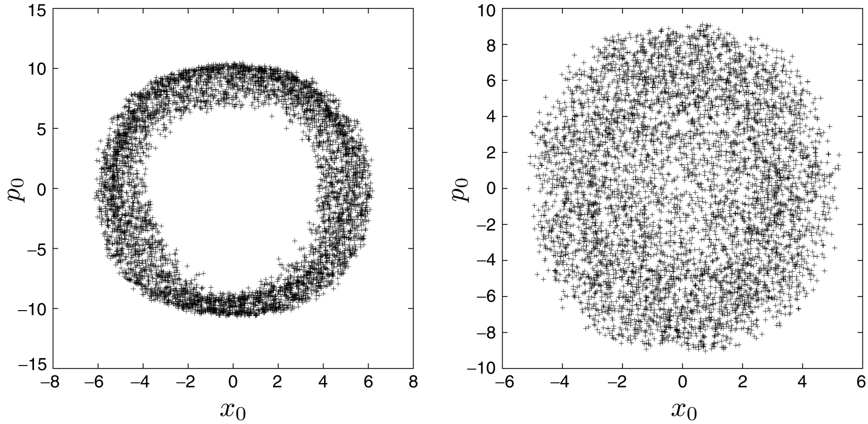

Figure 6. Plot of (x_0, p_0) with sampling period $1/\omega_0$ for the time interval $70,000 \leq t \leq 75,500$ (**left panel**) and for $20,000 \leq t \leq 25,500$ (**right panel**).

relatively large. In this case, the other modes, as well as the zeroth mode, show irregular, chaotic motions in energetically allowed regions.

As in the pioneering works, such as Ref. 12, we have confirmed that this many-dimensional model is a nonhyperbolic dynamical system, which has chaotic trajectories, along which motions change intermittently form irregular to ordered, and vice versa. However, it is not fully understood why we can find ordered motions just by monitoring relatively small local Lyapunov instability regions, although their magnitude itself has no relation to the orders of motions in principle.

B. Coexistence of Qualitatively Different Local Instabilities

When a continuous-time Hamiltonian system has an extra, independent conserved quantity, there exist a singular value increasing linearly in time and another singular value decreasing inversely proportional to time. Thus, when a system has an extra, independent quantity that is quasi-conserved during an finite time interval, such as ordered motion in Fig. 6 (left), there must exist a singular value increasing linearly in time and another singular value decreasing inversely proportional to time in the time interval.

Examples of typical plots of singular values $\mu_1(t, t_i)(= e^{\lambda_j(t,t_i)(t-t_i)})$ for ordered and irregular motions ($\Lambda = 2$, $\lambda = (32\pi)^{-1}$) are, respectively, the thick lines in Figs. 7a and 7b. These figures show that the local instability has a qualitative difference that corresponds to the orders of motions: μ_1 increases linearly in time, $t - t_i$, for (a) quasi-periodic ordered motions and exponentially for (b) irregular motions.

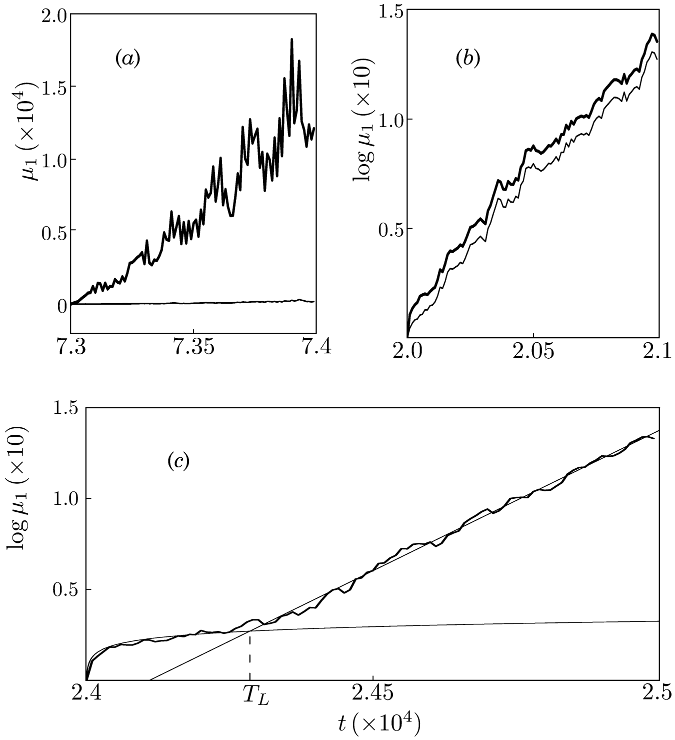

Figure 7. $\mu_1(t, t_i)$ against t, $t_i < t < t_i + 1000$, for an initial condition ($H(p(0), q(0)) = 300$): (a) $t_i = 73{,}000$ and (b) $t_i = 20{,}000$. The thick and the thin lines are our corrected results and the approximate results of the standard QR method, respectively. The thick line in (c) is μ_1 for $t_i = 24{,}000$. The thin lines are the fitted lines in the early linear and in the latter exponential stage, respectively. $T_L \sim 24{,}300$ is the time at the intersection of these fitted lines.

Moreover, thanks to the great accuracy of our method, lifetimes of ordered motions are preciously determined as follows. Figure 7c shows a typical plot of μ_1 that changes from linear to exponential increase. The crossover time T_L in Fig. 7c corresponds to the change from an ordered to an irregular motion. Thus the lifetime of the ordered motion is accurately given by T_L. Note that this method for computation of lifetimes has advantages over other more naive methods, such as direct presentation of trajectories with suitable variables, because it is applicable even when the values of T_L is too small to recognize their ordered motions or the choice of projected variables to visualize them is nontrivial.

Here we discuss the availability of conventional method for finding ordered motions. Suppose that a Hamilton system with N degrees of freedom has a number M ($M < N$) of quasi-conserved quantities I_j ($j = 1, 2, \ldots, M$). Then, each singular values that correspond to the quasi-conserved quantities I_j vary linearly and inverse linearly in time, and thus both of the associated finite-time Lyapunov exponents approach zero. The remaining singular values change exponentially and then the associated finite-time Lyapunov exponents approach nonzero finite values. Hence, for quasi-conserved quantities with sufficiently long lifetimes, their existence are shown by the finite-time Lyapunov exponents around zero. This is the case in which the conventional method, via relatively small instabilities in time series or the spectra, for detecting ordered motions are justified. In contrast, the singular value method presented here can find ordered motions, even when quasi-conserved quantities do not have long lifetimes enough to distinguish themselvs from nonzero value.

C. Correction in Many-Dimensional Systems

So far, the singular values have been computed by using our method with the relation $\mu_j = \exp(\lambda_j(t - t_i))$, where the accuracy is confirmed by comparing them to the result of the high-precision diagonalization of $M^T M$, as in Section III.C. Here, we show the indispensability of our novel corrections for acquiring the quantitative and qualitative properties.

The approximate μ_1 computed via the standard QR method are plotted for comparison, with the thin lines in Figs. 7a and 7b. These figures show that the standard QR method dose not have enough accuracy in both cases: (a) For ordered, quasi-periodic motions, the QR-approximate μ_1 gives much smaller result than the accurate result and does note give the original, linear increase. Hence, due to the absence of the exponential instability, the standard QR method fails to reproduce the *qualitative* change of μ_1. (b) For irregular chaotic motions, the approximate $\log \mu_1$ grows exponentially but is smaller by an approximately constant gap compared to the accurate result. Namely, the standard QR method fails to describe the quantitatively accurate change of $\log \mu_1$ in this case.

These also show that our corrections are necessary to obtain lifetimes of ordered motions, because, without these corrections, the qualitative changes, and thus the clear crossover times, generally disappear.

Thus, we have again confirmed that our corrections are necessary for accurate computation of local Lyapunov instability in this multidimensional dynamical system.

D. Summary

In this section, we have applied our novel method to the ϕ^4 model and clarified the following: (1) We give a new scheme for detecting ordered motions with the linear increase of singular values of stability matrixes. From the crossover times of local instabilities that change from linear to exponential increases, lifetimes of the associated ordered motions are determined accurately. (2) We then elucidated the condition that the conventional method for finding ordered motions are available. (3) The corrections are shown to be indispensable also for many-dimensional dynamical systems, in which magnitudes and directions of stable, unstable, and marginal Lyapunov instabilities may fluctuate.

V. CONCLUSION

In this chapter, we have developed a numerical algorithm for computing accurate values of finite-time Lyapunov exponents and vectors, by constructing a correcting procedure to the standard QR method. This procedure is a generalized LR method. As a result, the corrected results exponentially converge to the exact Lyapunov quantities for generic multidimensional dynamical systems including nonhyperbolic systems with (quasi-)degenerate Lyapunov spectra. This method is easy to implement [see Eqs. (19) and (36)] and very efficient, because of the exponential convergence and because the correcting procedure is called only when the exact quantities are necessary. We have demonstrated the efficiency of our method by applying it both to the standard map and to a multidimensional system consisting of oscillators. In the application to the latter system, alternations in qualitatively different local instabilities have been found along a trajectory. From crossover times of local instabilities that change from linear to exponential increases, lifetimes of the associated ordered motions are determined accurately.

We expect that this correcting procedure can be applicable for other numerical methods, such as the symplectic method [21,22], and that faster convergence may be accomplished by introducing shifts [18] into the correcting process. These variants would be useful for exploring instability, especially, in high-dimensional dynamical systems. We hope that these methods will help us to develop understandings of generic multidimensional nonhyperbolic chaotic systems.

Acknowledgments

I express gratitude to A. Shudo and A. Tanaka for continuous encouragement and enlightening discussions. The support given by the following sponsors is deeply appreciated: the Japan–U.S. Cooperative Science Program of Japan Society of the Promotion of Science, Inoue Foundation for Science, and Yukawa Institute for Theoretical Physics at Kyoto University.

References

1. J.-P. Eckmann and D. Ruelle, *Rev. Mod. Phys.* **57**, 617 (1985).
2. M. Sano and Y. Sawada, *Phys. Rev. Lett.* **55**, 1082 (1985).
3. T. D. Sauer, J. A. Tempkin, and J. A. Yorke, *Phys. Rev. Lett.* **81**, 4341 (1998).
4. T. D. Sauer and J. A. Yorke, *Phys. Rev. Lett.* **83**, 1331 (1999).

5. H. D. I. Abarbenel, *Analysis of Observed Chaotic Data*, Springer-Verlag, New York, 1995.
6. A. J. Lichtenberg and M. A. Lieberman, *Regular and Stochastic Motion*, Springer-Verlag, New York, 1983.
7. E. Ott, *Chaos in Dynamical Systems*, Cambridge University Press, Cambridge, 1993.
8. V. I. Oseledec, *Moscow Math. Soc.* **19**, 197 (1968).
9. I. Goldhirsch, P.-L. Sulem, and S. A. Orszag, *Physica D* **27**, 311 (1987).
10. Y. Aizawa, Y. Kikuchi, T. Harayama, K. Yamamoto, M. Ota, and K. Tanaka, *Prog. Theor. Phys. Suppl.* **98**, 36 (1989).
11. M. A. Sepúlveda, R. Badii, and E. Pollak, *Phys. Rev. Lett.* **63**, 1226 (1989).
12. T. Konishi and K. Kaneko, *J. Phys. A* **25**, 6283 (1991).
13. T. Morita, H. Hata, H. Mori, T. Horita, and K. Tomita, *Prog. Theor. Phys.* **79**, 296 (1988).
14. S. Dawson, C. Grebogi, T. Sauer, and J. A. Yorke, *Phys. Rev. Lett.* **73**, 1927 (1994); T. Sauer, C. Grebogi, and J. A. Yorke, *Phys. Rev. Lett.* **79**, 59 (1997).
15. W. B. Hayes, *Phys. Rev. Lett.* **90**, 54104 (2003).
16. X. Z. Tang and A. H. Boozer, *Physica D* **95**, 283 (1996); M. M. Alvarez, F. J. Muzzio, S. Cerbelli, A. Adrover, and M. Giona, *Phys. Rev. Lett.* **81**, 3395 (1998); M. Giona and A. Adrover, *Phys. Rev. Lett.* **81**, 3864 (1998); A. Adrover and M. Giona, *Phys. Rev. E* **60**, 347 (1999); J.-L. Thiffeault and A. H. Boozer, *Chaos* **11**, 16 (2001); M. Giona, S. Cerbelli, and A. Adrover, *Phys. Rev. Lett.* **88**, 024501 (2002).
17. K. Geist, U. Parlitz, and W. Lauterborn, *Prog. Theor. Phys.* **83**, 875 (1990).
18. G. H. Golub and C. F. Van Loan, *Matrix Computations*, 3rd ed., Johns Hopkins University Press, Baltimore, 1996.
19. G. Benettin, L. Galgani, and J. M. Strelcyn, *Phys. Rev. A* **14**, 2338 (1976); I. Shimada and T. Nagashima, *Prog. Theor. Phys.* **61**, 1605 (1979).
20. F. Christiansen and H. H. Ruth, *Nonlinearity* **10**, 1063 (1997).
21. S. Habib and R. D. Ryne, *Phys. Rev. Lett.* **74**, 70 (1995); G. Rangarajan, S. Habib, and R. D. Ryne, *Phys. Rev. Lett.* **80**, 3747 (1998).
22. M. H. Partovi, *Phys. Rev. Lett.* **82**, 3424 (1999).
23. J.-L. Thiffeault, *Physica (Amsterdam)* **172D**, 139 (2002).
24. T. Okushima, *Phys. Rev. Lett.* **91**, 254101 (2003)